19th International Conference on
Adaptive Structures and Technologies
October 6-9, 2008
Ascona, Switzerland

Analysis of Passive Vibration Suppression System Comprising Piezoelectric Elements

Hiroshi Okubo[1]* and Nagisa Shimazaki[1]
[1] Osaka Prefecture University, Japan
1-1 Gakuen-cho, Sakai, Osaka, 599-8531 Japan, +81-72-254-9242, +81-72-254-9906, okubo@aero.osakafu-u.ac.jp

ABSTRACT

In this study, a passive vibration suppression system comprising piezoelectric elements is developed for flexible structures. The vibration suppression system comprises a cantilevered beam with bimorph piezoelectric ceramic tiles shunted by an RL electrical circuit. A general design method for the vibration suppression of the beam is theoretically analyzed using the mode analysis assuming that the piezoelectric elements are sufficiently thin and do not change the mode shape of the beam. Under this assumption, the vibration suppression system for the beam could be designed by tuning the resistance and inductance parameters of the shunted RL network. As an example, numerical simulations are carried out for a cantilevered beam, and the results are verified experimentally. The results of the numerical simulations and the vibration control experiment show that the passive vibration suppression system is practically effective in damping vibrations. This study shows that electrical systems function as a type of a dynamic damper for mechanical systems, and it is quite effective to optimize the resistance, as well as the inductance, of the passive electrical network to suppress the peak gain of the response transfer function over the resonant frequency range.

Keywords: Smart Structures, Piezoelectric Elements, Passive Vibration Suppression

1. INTRODUCTION

In the recent years, smart structures in which piezoelectric elements are used as embedded sensors and actuators and as elements of active structural vibration suppression systems have been studied. Two types of piezoelectric control systems are used for vibration damping, i.e., active and passive control systems. Active control systems require complex amplifiers and associated sensing electronics, whereas passive control systems require only a simple passive electrical circuit. Moreover, passive control systems are more effective in vibration damping with limited resources, such as in the case of space applications.

Piezoelectric materials strain when an electrical field is applied across them, which makes them suitable for application as actuators in control systems. Further, they also produce voltage when subjected to strain, as a result of which they can be used for sensing strains. In general, piezoelectrics can efficiently transform mechanical energy into electrical energy and vice versa and, therefore, can be used as structural dampers [1]. The modeling of passive dampers by using piezoelectric elements along with shunted circuits has been reported by several literatures [2, 3].

In this study, a dynamic model is developed for structures with passive damping mechanism and piezoelectric elements. The efficiency of passive vibration damping is estimated according to the optimal tuning theory assuming that the mass and stiffness of the piezoelectric elements are small as compared to those of the beam so that the variations in the eigenfrequencies and mode shapes are

negligible. The passive vibration suppression system is used for damping the vibrations of a cantilevered smart beam, and the results of the numerical simulations are compared with those obtained experimentally.

2. MODELING OF PASSIVE PIEZOELECTRIC DAMPERS

2-1. Constitutive equations

Figure 1 shows a typical piezoelectric element. The fundamental constitutive relations are the relations between strain and applied field and between the charge density and the applied strain.

$$D_3 = \epsilon_{33}^{\mathsf{T}} \cdot E_3 + d_{31} \cdot T_1 \tag{1}$$

$$S_1 = d_{31} \cdot E_3 + s_{11}^{\mathsf{E}} \cdot T_1 \tag{2}$$

where S_1 and T_1 denote the applied strain and stress in the x-direction, respectively; E_3 and D_3, the applied electric field and charge density in the y-direction, respectively; and s^{E}_{11}; d_{31}, and $\epsilon_{33}^{\mathsf{T}}$, the elastic compliance in the x-direction, piezoelectric constant, and dielectric constant, respectively.

E_3 and D_3 are replaced by the voltage V_3 and the current I_3 in the following relations, respectively:

$$V_3 = hE_3 \tag{3}$$

$$I_3 = s \cdot l_{\mathsf{p}} \epsilon_{33}^{\mathsf{T}} / t_{\mathsf{p}} \tag{4}$$

where s is the Laplace parameter. The inherent capacitance of the shunted piezoelectric is given as

$$C_{\mathsf{p}}^{\mathsf{T}} = \frac{w l_{\mathsf{p}} \epsilon_{33}^{\mathsf{T}}}{t_{\mathsf{p}}} \tag{5}$$

The constitutive equation can be given as

$$I_3 = sC_{\mathsf{p}}^{\mathsf{T}} \cdot V_3 + sAd_{31} \cdot T_1 \tag{6}$$

$$S_1 = d_{31}/t_{\mathsf{p}} \cdot V_3 + s_{11}^{\mathsf{E}} \cdot T_1 \tag{7}$$

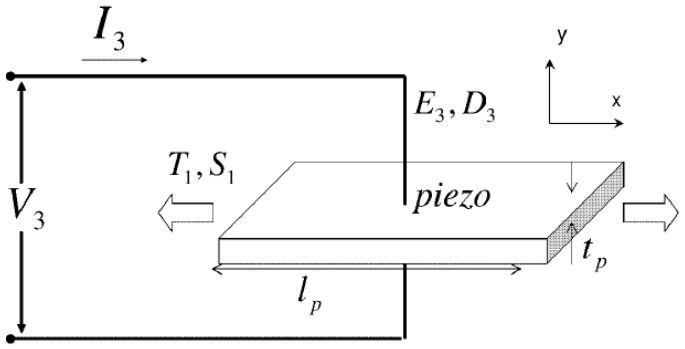

Figure 1. Piezoelectric element with potential difference applied across top and bottom surfaces

2-2. Resonant circuit shunting

Consider a resonant circuit and shunt the inherent capacitance of the piezoelectric element using a resistor and an inductor in series, thereby forming an LCR circuit. This circuit is shown in Fig. 2. In this case, the electrical impedance Z_{EL} of the entire circuit including the piezoelectric element is given by

$$Z_{\mathsf{EL}}(s) = \frac{Ls + R}{LC_{\mathsf{p}}^{\mathsf{T}} s^2 + RC_{\mathsf{p}}^{\mathsf{T}} s + 1} \tag{8}$$

where L is the shunting inductance and R is the shunting resistance. This circuit is resonant with some damping due to the resistance, R. and it can be tuned in the vicinity of a mode of the underlying mechanical system and thereby greatly increase the modal damping ratio, in an effect similar to the classical proof mass damper (PMD) or resonant vibration absorber.

The constitutive equation of piezoelectrics with a resonant passive circuit is given by

$$I_3 = Z_{\mathsf{EL}}(s)^{-1} \cdot V_3 + sAd_{31} \cdot T_1 \tag{9}$$

$$S_1 = d_{31}/t_{\mathsf{p}} \cdot V_3 + s_{11}^{\mathsf{E}} \cdot T_1 \tag{10}$$

where the electrical impedance of the open loop $Z^{\mathsf{D}}(s) = 1/sC_{\mathsf{P}}^{\mathsf{T}}$ is replaced by the total electrical impedance of the shunted circuit $Z_{EL}(s)$. The relation between S_1, T_1, and I_3 can be given from Eqs. (9) and (10) as follows:

$$S_1 = \left(s_{11}^{\mathsf{E}} - \frac{d_{31}^2 A}{t_{\mathsf{p}}} s \cdot Z_{\mathsf{EL}}(s) \right) T_1 + \frac{d_{31}}{t_{\mathsf{p}}} Z_{\mathsf{EL}}(s) \cdot I_3 \tag{11}$$

Since there is no external input current ($I_3 = 0$) in passive shunting applications, the compliance s_{11}^{SU} that relates S_1 and T_1 can be expressed by using the nondimensional electrical impedance $\bar{Z}_{\mathsf{EL}}(s) = Z_{\mathsf{EL}}(s)/Z_{\mathsf{D}}(s) = Z_{\mathsf{EL}} \cdot sC_{\mathsf{P}}^{\mathsf{T}}$ as

$$s_{11}^{\mathsf{SU}} = s_{11}^{\mathsf{E}} - \frac{d_{31}^2 A}{t_{\mathsf{P}}} s \cdot Z_{\mathsf{EL}}(s) = s_{11}^{\mathsf{E}} \left(1 - k_{31}^2 \bar{Z}_{\mathsf{EL}}(s)\right) \tag{12}$$

where k_{31} denotes the electromechanical coupling constant of the piezoelectric material and is defined as

$$k_{31}^2 = \frac{d_{31}^2}{s_{11}^{\mathsf{E}} \epsilon_{33}^{\mathsf{T}}} \tag{13}$$

k_{31} represents the ratio of electrical energy and mechanical energy that can be stored in piezoelectric elements.

Equation (12) shows that the compliance of the shunted piezoelectric is equal to the short-circuit compliance of the piezoelectric material modified by a term that depends on the electrical shunt circuit and the electromechanical coupling coefficient of the piezoelectric material.

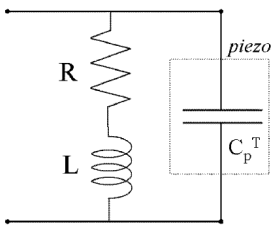

Figure 2. Resonant shunted piezoelectric with resistor and inductor in series

3. OPTIMAL DESIGN OF PASSIVE PIEZOELECTRIC DAMPERS

3-1. Finite element modeling of dynamical system

Consider a finite element model of a cantilevered beam with piezoelectric elements attached on both its surfaces, as shown in Fig. 3. The undamped equation of motion of the beam is expressed as

$$[M]\{\ddot{q}\} + [K]\{q\} = \{F\} \tag{14}$$

where M and K are the mass, stiffness, and damping matrices, respectively. The deflection $\{q\}$ and external force $\{F\}$ are the vectors of the transverse deflections w_i , angular deflections θ_i, forces F_i, and moments M_i of each node.

$$\{q\} = \{w_1, \theta_1, \cdots w_i, \theta_i, \cdots w_N, \theta_N\}^T \tag{15}$$

$$\{F\} = \{F_1, M_1, \cdots F_i, M_i, \cdots F_N, M_N\}^T \tag{16}$$

By introducing the modal coordinate transformation

$$\{q\} = [\Phi]\{z\} = \{\phi_1\}z_1 + \{\phi_2\}z_2 + \cdots + \{\phi_N\}z_N \tag{17}$$

the equation of motion of the system can be transformed into the following modal form:

$$\begin{bmatrix} m_1 & & \\ & \ddots & \\ & & m_N \end{bmatrix}\{\ddot{z}\} + \begin{bmatrix} k_1 & & \\ & \ddots & \\ & & k_N \end{bmatrix}\{z\} = [\Phi]^T\{F\} \tag{18}$$

where $\{z\} = \{z_1, z_2, \cdots z_N\}^T$ denotes the vector of the modal coordinate s; $[\Phi] = [\{\phi_1\}, \{\phi_2\} \cdots, \{\phi_N\}]$, the modal matrix; $m_i = \{\phi_i\}^T[M]\{\phi_i\}$, the i-th modal mass; and $k_i = \{\phi_i\}^T[K]\{\phi_i\}$, the i-th modal stiffness.

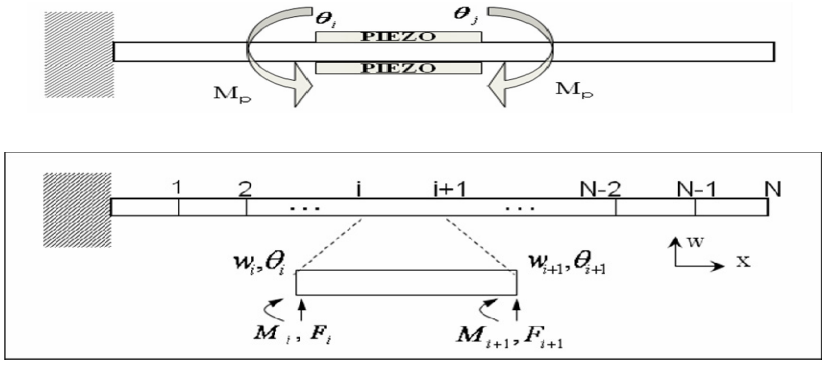

Figure 3. Finite element model of cantilevered beam with piezoelectric elements

3-2. Modeling of feedback force of piezoelectric elements

It is assumed that the mass and stiffness of the piezoelectric elements are small and do not affect the mode shape of the beam. It is also assumed that a bending moment applied to the beam causes a constant variation in the deflection angle between the ends of the piezoelectrics as follows:

$$\frac{d\theta}{dx} = \frac{\theta_{\mathrm{j}} - \theta_{\mathrm{i}}}{l_{\mathrm{P}}} \tag{19}$$

Then, the couple of bending moments provided by the piezoelectric elements can be given as

$$M_{\mathrm{P}} = -Ep(s) I_{\mathrm{P}} \frac{d\theta}{dx} = -Ep(s) I_{\mathrm{P}} \frac{\theta_{\mathrm{j}} - \theta_{\mathrm{i}}}{l_{\mathrm{P}}} \tag{20}$$

where I_{P} is the moment of inertia of both the piezoelectrics and E_p is the frequency-dependent Young's modulus of the piezoelectric elements that can be described as the inverse of the mechanical compliance, i.e., $E_p(s) = 1/s_{11}(s)$.

The piezoelectric bending moment M_{P} is introduced into the equation of motion as the feedback force. It can be represented by using a displacement vector as

$$\begin{aligned} M_{\mathrm{P}} &= -Ep(s) \frac{I_{\mathrm{P}}}{l_{\mathrm{P}}} \{\cdots -1 \cdots 1 \cdots\} \{\cdots \theta_{\mathrm{i}} \cdots \theta_{\mathrm{j}} \cdots\}^{\mathsf{T}} \\ &= -Ep(s) \frac{I_{\mathrm{P}}}{l_{\mathrm{P}}} \{\cdots -1 \cdots 1 \cdots\} \{q\} \end{aligned} \tag{21}$$

The feedback force vector can be given as

$$\begin{aligned} \{F_{\mathrm{d}}\} &= \{\cdots -M_{\mathrm{P}} \cdots M_{\mathrm{P}} \cdots\}^{\mathsf{T}} \\ &= -Ep(s) \frac{I_{\mathrm{P}}}{l_{\mathrm{P}}} \{\cdots -1 \cdots 1 \cdots\}^{\mathsf{T}} \{\cdots -1 \cdots 1 \cdots\} \{q\} \end{aligned} \tag{22}$$

If we consider a single vibration mode, e.g., the first mode, the modal feedback force can be given as follows:

$$\begin{aligned} \{\phi_1\}^{\mathsf{T}} \{F_{\mathrm{d}}\} &= -Ep(s) \frac{I_{\mathrm{P}}}{l_{\mathrm{P}}} \{\phi_1\}^{\mathsf{T}} \{\cdots -1 \cdots 1 \cdots\}^{\mathsf{T}} \{\cdots -1 \cdots 1 \cdots\} \{\phi_1\} z_1 \\ &= -Ep(s) \frac{I_{\mathrm{P}}}{l_{\mathrm{P}}} (\phi_{1\mathrm{j}} - \phi_{1\mathrm{i}})^2 \cdot z_1 \end{aligned} \tag{23}$$

Therefore, the equation of motion for the first mode including the feedback force of the piezoelectric elements is written as

$$\{\phi_1\}^{\mathsf{T}} [M] \{\phi_1\} \ddot{z}_1 + \{\phi_1\}^{\mathsf{T}} [K] \{\phi_1\} z_1 = \{\phi_1\}^{\mathsf{T}} (\{Fd\} + \{F\})$$

$$m_1 \ddot{z}_1 + k_1 z_1 + Ep(s) \frac{I_{\mathrm{P}}}{l_{\mathrm{P}}} (\phi_{1\mathrm{j}} - \phi_{1\mathrm{i}})^2 \cdot z_1 = F_1 \tag{24}$$

where m_1 and k_1 are the modal mass and modal stiffness, respectively, in the case of the first mode and F_1 is the modal force. The Laplace transform of the abovementioned equation gives the transfer function of the modal coordinate.

$$z_1 = \frac{F_1}{m_1 s^2 + k_1 + Ep(s) \frac{I_{\mathrm{P}}}{l_{\mathrm{P}}} (\phi_{1\mathrm{j}} - \phi_{1\mathrm{i}})^2} \tag{25}$$

3-3. Optimal tuning problem

The Young's modulus *E*p(s) of the piezoelectric elements with the resonant shunt circuit is given as

$$E_{\mathrm{P}}(s) = \frac{1}{s_{11}^{\mathrm{SU}}} = E_{\mathrm{P}}^{\mathrm{E}} \cdot \frac{1}{1 - k_{31}^2 \bar{Z}_{\mathrm{EL}}(s)} \tag{26}$$

$$\bar{Z}_{\mathrm{EL}}(s) = \frac{Ls^2 + Rs}{Ls^2 + Rs + 1/C_{\mathrm{p}}^{\mathrm{T}}} \tag{27}$$

where $E_{\mathrm{P}}^{\mathrm{E}} = 1/s_{11}^{\mathrm{E}}$ is the elastic modulus of the shorted circuit. Substituting Eq. (26) into Eq. (25), the transfer function of the modal displacement can be given as

$$z_1 = \frac{F_{1\mathrm{p}}}{m_{1\mathrm{p}} s^2 + k_{1\mathrm{p}} + Ep(s)} \tag{28}$$

where the new parameters $F_{1\mathrm{P}}$, $m_{1\mathrm{P}}$, and $k_{1\mathrm{P}}$ are normalized by $I_{\mathrm{P}}/L_{\mathrm{P}} \cdot (\phi_{1\mathrm{j}} - \phi_{1\mathrm{i}})^2$.

The nondimensional transfer function is given as follows [2]:

$$\frac{z_1}{z_{\mathrm{ST}}} = \frac{\gamma^2 + \delta^2 + \delta^2 r\gamma}{(\gamma^2 + 1)(\gamma^2 + \delta^2 + \delta^2 r\gamma) + K_{31}^2(\gamma^2 + \delta^2 r\gamma)} \tag{29}$$

where the nondimensional parameters are defined as follows:

$\omega_1^{\mathrm{E}} = \sqrt{(k_{1\mathrm{p}} + E_{\mathrm{P}}^{\mathrm{E}})/m_{1\mathrm{p}}}$: natural frequency

$\gamma = s/\omega_1^{\mathrm{E}}$: nondimensional frequency

$r = RC_{\mathrm{P}}^{\mathrm{S}}\omega_1^{\mathrm{E}}$: electrical damping ratio

$\omega_{\mathrm{e}} = 1/\sqrt{LC_{\mathrm{P}}^{\mathrm{S}}}$: resonant shunted piezoelectric electrical resonant frequency

$\delta = \omega_{\mathrm{e}}/\omega_1^{\mathrm{E}}$: resonant shunted piezoelectric frequency tuning parameter

$C_{\mathrm{P}}^{\mathrm{S}}$ denotes the capacitance at constant strain, $C_{\mathrm{P}}^{\mathrm{S}} = C_{\mathrm{P}}^{\mathrm{T}}(1 - k_{31}^2)$, and K_{31} and z_{ST} are the generalized electromechanical coupling coefficient and static displacement, respectively.

$$K_{31}^2 = \frac{E_{\mathrm{P}}^{\mathrm{E}}}{k_{1\mathrm{p}} + E_{\mathrm{P}}^{\mathrm{E}}} \cdot \frac{k_{31}^2}{1 - k_{31}^2} \tag{30}$$

$$z_{\mathrm{ST}} = \frac{F_{1\mathrm{p}}}{k_{1\mathrm{p}} + E_{\mathrm{P}}^{\mathrm{E}}} \tag{31}$$

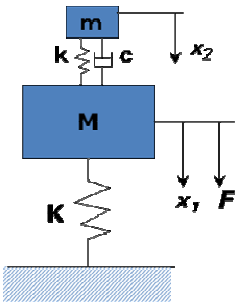

Equation of Motion

$$M\ddot{x}_1 + c(\dot{x}_1 - \dot{x}_2) + Kx_1 + k(\dot{x}_1 - \dot{x}_2) = F$$
$$m\ddot{x}_2 + c(\dot{x}_2 - \dot{x}_1) + k(\dot{x}_2 - \dot{x}_1) = 0$$

Transfer Function

$$\frac{x_1}{F} = \frac{1}{Ms^2 + K + \left(\frac{(cs+k)ms^2}{ms^2 + cs + k}\right)}$$

Figure 4. Mechanical proof mass damper (PMD)

It has been shown in a study [2, 3] that the similarities between a system containing resonant shunted piezoelectrics (RSPs) and a system containing a mechanical vibration absorber or a PMD can be used for the optimal tuning and damping of the electrical circuit of RSPs. Figure 4 shows the PMD and the displacement transfer function that includes a resonant vibration absorber similar to the RSPs. The optimal tuning parameters of the resonant shunted piezoelectrics are obtained as outlined in references and the optimal inductance and resistance of the resonant circuit are given as

$$L_{\text{opt}} = \frac{1}{\omega_1^{E2}\, C_P^S} \cdot \frac{1}{1+K_{31}^2} \tag{32}$$

$$R_{\text{opt}} = \frac{1}{\omega_1^{E}\, C_P^S} \cdot \frac{\sqrt{2}K_{31}}{1+K_{31}^2} \tag{33}$$

4. APPLICATION TO CANTILEVERED BEAM

4-1. Numerical simulations

Numerical simulations and dynamic tests were performed on the cantilevered beam with piezoceramics stuck to its surfaces. The cantilevered beam with the resonant shunted piezoceramics is shown in Fig. 5. The length, width, and thickness of the cantilevered beam was 45.00 cm, 3.00 cm, and 0.3 mm, respectively. A couple of surface-mounted piezoceramics were attached to both sides of the beam and shunted by using an RL resonant circuit. The shunted pair consisted of 0.2-mm-thick C-6 piezoceramic sheets manufactured by Fuji Ceramics Co., Inc. The specifications of the beam and the piezoceramics are presented in Table 1.

The natural frequencies of the bare beam for the first and second modes were $\omega_1 = 7.70$ rad/sand $\omega_2 = 48.24$ rad/s, respectively. The numerical simulations were carried out for three different positions of the piezoelectric elements, i. e., (1) root, (2) middle, and (3) tip. The optimal parameters for the first vibration mode obtained by using Eqs. (32) and (33) are listed in Table 2. Figure 6 shows the impulse responses and Bode gain plots for the three different positions of the piezoelectric elements.

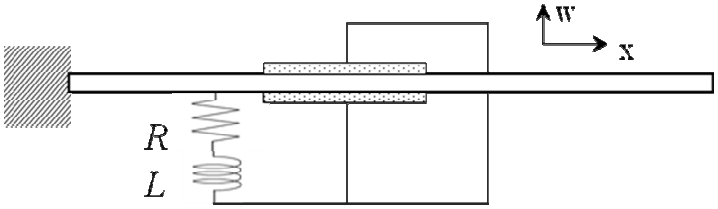

Figure 5. Model of cantilevered beam with resonant shunted piezoelectrics (RSPs)

Table 1. Specifications of beam and piezoceramics

Beam	Length	4.50×10^{-1}(m)
	Width	3.00×10^{-2}(m)
	Thickness	3.00×10^{-4}(m)
	Density	$7.86\times 10^{3}(\frac{kg}{m^3})$
	Young's modulus	$206\times 10^{9}(\frac{N}{m^2})$
Piezo elements	Length	3.00×10^{-2}(m)
	Width	3.00×10^{-2}(m)
	Thickness	2.00×10^{-4}(m)
	Density	$7.40\times 10^{3}(\frac{kg}{m^3})$
	Young's modulus	$58.0\times 10^{9}(\frac{N}{m^2})$
	Piezoelectric constant	$-1.95\times 10^{-10}(\frac{m}{V})$

Table 2. Optimal parameters of RSPs

		$L_{opt}[H]$	$R_{opt}[\Omega]$
(1)	Root $= 2.5 \sim 32.5$ [mm]	1.100×10^5	6.920×10^5
(2)	Middle $= 210 \sim 240$	2.740×10^5	6.199×10^5
(3)	Tip $= 420 \sim 450$	3.518×10^5	5.963×10^3

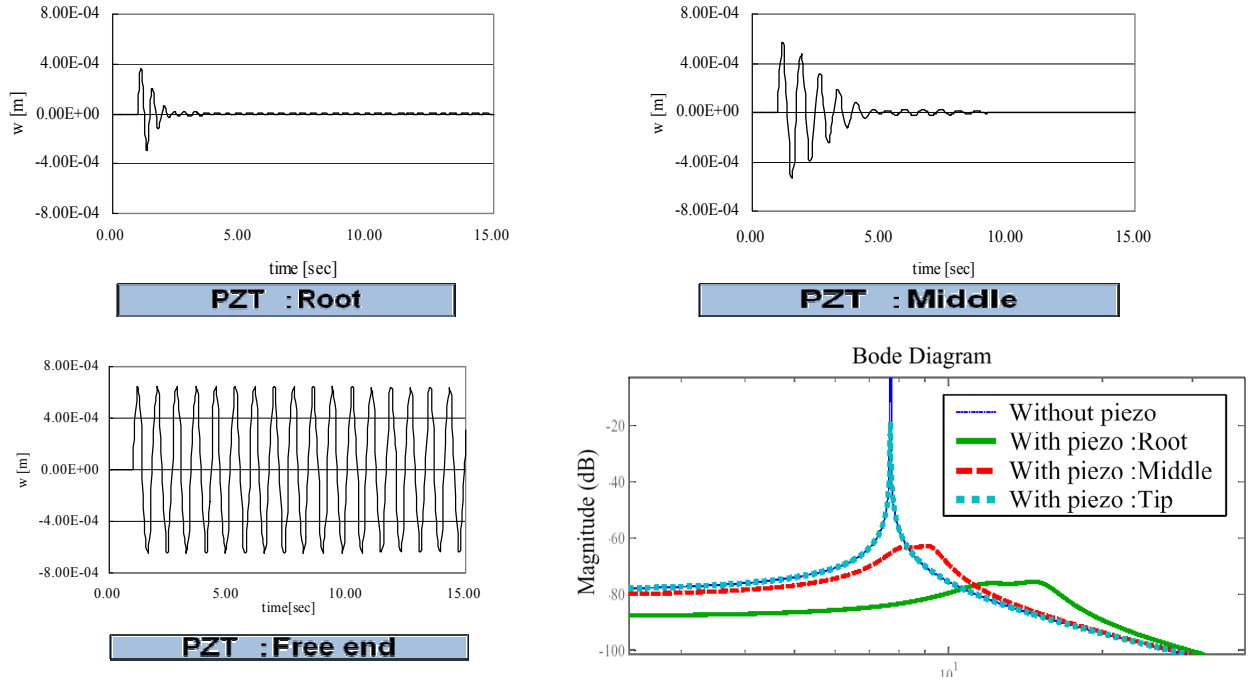

Figure 6. Responses for various positions of piezoelectric elements

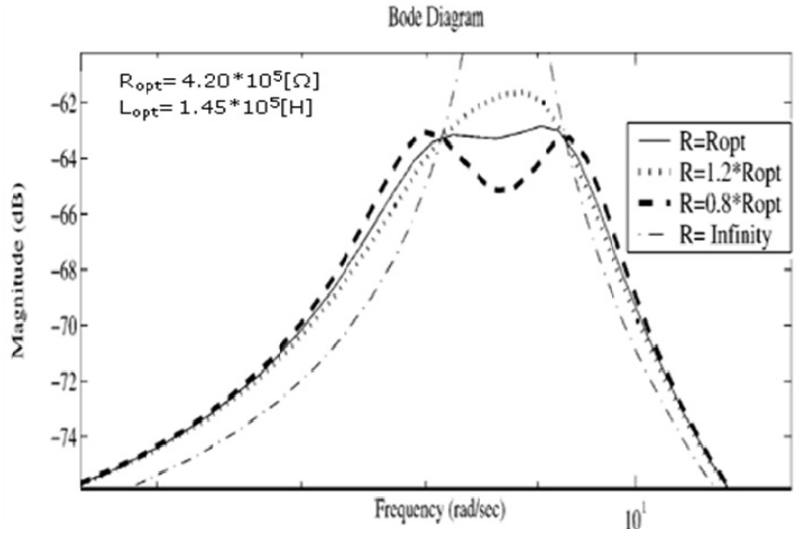

Figure 7. Bode diagrams at optimal frequency tuning and various resistance values: (solid) optimal resistance tuning, $R = R_{opt}$; (dotted) $R = 1.2R_{opt}$; and (dashed) $R = 0.8R_{opt}$

The Bode gain plots of the displacement of the tip of the cantilevered beam for various values of resistances when the piezoceramic sheets are placed at the root of the beam are presented in Fig. 7. These plots are very similar to the transfer functions for a 1-DOF system containing a PMD for various values of damping parameters. This similarity shows that the resistance of the RSPs functions as a damper of the PMD.

4-2. Experimental results

The results of a laboratory experiment [4] were compared with those of the numerical simulations in order to verify the validity of the analytical formulae for shunted piezoelectrics. An uncorrelated pseudo-random input was used to excite the beam near its first bending mode, and the displacement of the tip of the beam was measured. (Figures 8 and 9) The amplified displacement signal was collected and a transfer function from the input voltage to strain was computed. The values of the resistor and inductor were tuned to the first bending mode, according to Eqs. (32) and (33). Since the first mode frequency was very low for the experimental beam, a large inductance (L_{opt} = 173.1 kH) was required for the resonant shunt circuit. During the experiment, the circuit of the resistor and inductor in series was replaced by a synthetic inductor consisting of an operational amplifier and a CR circuit shown in Fig. 10.

The transfer function from the input voltage to the displacement is shown in Fig. 11. The resistance was further varied in the range of the optimal value to validate the behavior of the resonant shunted piezoelectric system in response to parameter changes. The characteristics of the numerical and experimental results were similar. This similarity shows that the analytical model of the shunted piezoelectrics can be used valid for estimating the performance of the passive RSP damper.

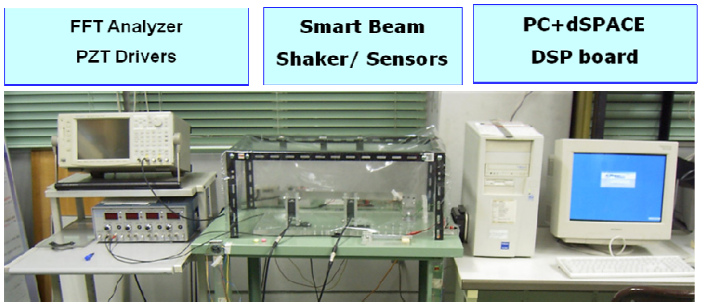

a) Overview of experimental system

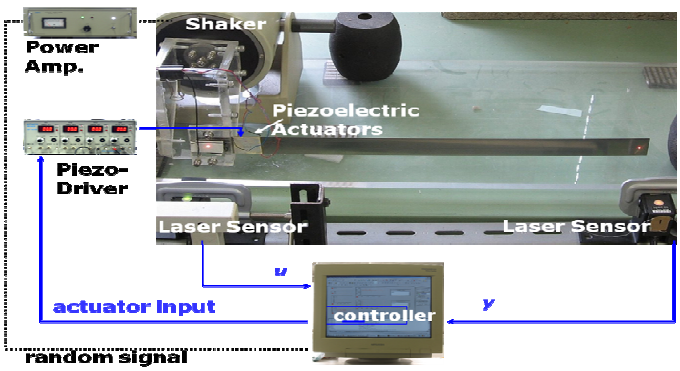

b) Block diagram of sensory and measurement systems

Figure 8. Experimental setup for laboratory experiment

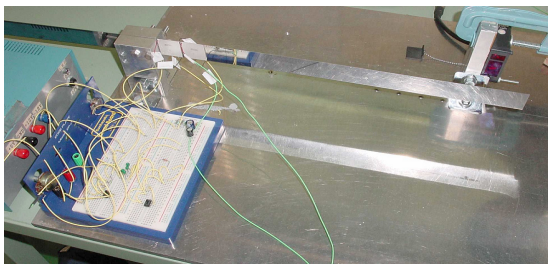

Figure 9. Experimental shunt circuit of passive piezoelectric damper

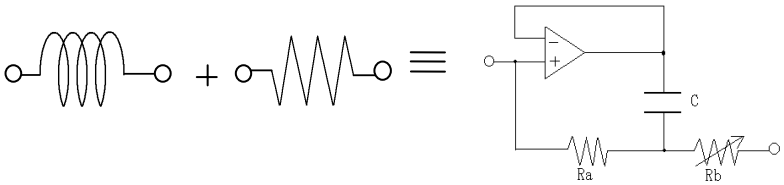

Figure 10. Synthetic inductor substituted for RL series circuit

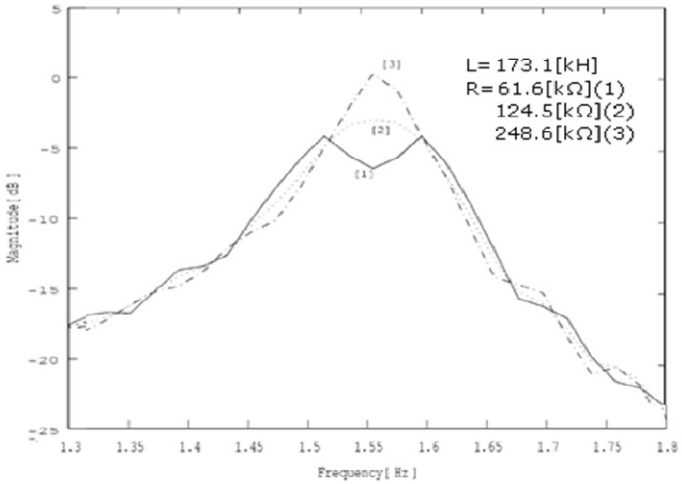

Figure 11. Experimental transfer functions at optimal frequency tuning for various resistance values: (solid) optimal resistance tuning, R = 61.6 kΩ; (dotted) R = 124.5 kΩ; and (dot-dashed) R = 248.6 kΩ

4. CONCLUSIONS

A passive vibration suppression system has been developed for flexible structures. A finite element model of a flexible beam with piezoelectric elements has been developed. The dynamics of the beam with resonant shunted piezoelectrics (RSPs) is analyzed assuming that the mass and stiffness of the piezoelectric elements are small as compared to those of the beam. The response transfer function of the beam with RSPs is similar to that of a system containing a mechanical vibration absorber or a proof mass damper (PMD), and the classical tuning theory can be used for the optimal tuning of the circuit parameters of the RSPs.

The effectiveness of the passive damping system with RSPs has been shown by numerical simulations and by carrying out an experiment using a cantilevered smart beam. The results of the numerical simulation show that the electrical system functions as a type of dynamic damper for the mechanical system, and it is quite effective to design the optimal parameters of the passive electrical network to suppress the peak gain over the resonant frequency range.

REFERENCES

1. Uchino, K., Piezoelectric/Electrorestrictive Actuators, Morikita Publishing Co., Ltd., (1986). [in Japanese]
2. Hagood, N. W. and A. Von Flotow, "Damping of structural vibrations with piezoelectric materials and passive electrical networks," *Journal of Sound and Vibration*, Vol. 146, No. 2, pp. 243–268 (1991).
3. Fujita, T. et al., "Fundamental Study of Passive Microvibration Control with Smart Structure Using Piezoelectric Devices," *Trans. JSME*, Vol. C-66, No. 644, pp. 1097–1101 (2000). [in Japanese]
4. Koike, T. and H. Okubo, "Passive Vibration Suppression System Using Piezoelectric Elements," *JSME Dynamics and Design Conference*, Paper 427, pp. 1–6 (2001). [in Japanese]